https://doi.org/10.5194/wes-2026-138
Preprint. Discussion started: 3 September 2026

WIND ENERGY SCIENCE DISCUSSIONS
Open Access

Brief communication: On the local disagreement of two engineering models for the radial induced velocity of non-planar wind turbine rotors

Alois Peter Schaffarczyk and Bhima Masare
Kiel University of Applied Sciences, Mechanical Engineering, D-24149 Kiel, Germany
Correspondence: alois.schaffarczyk@haw-kiel.de

Abstract. Blade element momentum (BEM) codes traditionally neglect the radial induced velocity u_r, although for the strongly deflected or prebent blades of current multi-MW turbines it produces an additional in-plane driving force. Two engineering models proposed by Li et al. (2022) — the smooth correction attributed to Madsen, driven by the area-averaged thrust coefficient, and the superposition of discrete semi-infinite vortex cylinders formed from the converged annulus inductions — were implemented independently in an open-source blade design and analysis code. For the NREL 5 MW reference rotor with an operational tip deflection of 6 m both models change thrust and power by less than 1 %, and their integral effects on the power coefficient agree to within 0.05 %. This agreement conceals a pronounced local disagreement: at mid-span the vortex-cylinder u_r changes sign, following the non-monotonic radial derivative of the axial induction, and at the outermost section it grows logarithmically with the number of blade sections, $u_r \simeq 0.78 \ln N_{sec} + 3.05$ ($\mathrm{m\,s^{-1}}$), in close agreement with the analytic slope $|\gamma_t^{tip}|/2\pi = 0.82$, reaching $6.6\,\mathrm{m\,s^{-1}}$ at $N_{sec} = 70$ against $2.3\,\mathrm{m\,s^{-1}}$ for the Madsen correction. We show that the integral agreement is systematic rather than coincidental, and that local load predictions near the tip of non-planar rotors are model- and grid-dependent and require an explicit, resolution-independent regularisation.

1 Introduction

The blade element momentum (BEM) method remains the work horse of applied wind turbine aerodynamics. In its classical form (Glauert, 1935) the rotor is planar and only the axial and circumferential induced velocities enter the force balance. Modern rotor blades, however, operate with substantial out-of-plane (oop) deflections — of the order of 10 % of the tip radius — and are increasingly designed with prebend and sweep. For such non-planar rotors the radial induced velocity u_r, which accompanies wake expansion, is no longer orthogonal to the local blade section: it produces an additional in-plane (driving or braking) force proportional to $\tan\kappa$, where κ is the local cone angle of the deflected blade.

Li et al. (2022) presented a consistent, computationally efficient framework for this effect and proposed a hierarchy of models, from a simple engineering correction attributed to Madsen (see also Madsen et al. (2020)) up to a coupled solution using the cylindrical vortex wake model of Branlard and Gaunaa (2015). Two members of this hierarchy were implemented independently in the open-source blade design and analysis code KSS (Schaffarczyk et al., 2022): (i) the Madsen correction and (ii) an uncoupled vortex-cylinder (VC) superposition. The purpose of this brief communication is to report a practically relevant observation made in this exercise: the two models agree almost perfectly in their integral effect while disagreeing strongly — qualitatively, not just quantitatively — in the local distribution of u_r, and the discrete VC model is shown to be grid-dependent at the tip, with a numerically verified logarithmic divergence. Both facts matter when such models are used for local load predictions, e.g. in aeroelastic tailoring of blade tips.

2 Models and implementation

Both models act as a post-convergence correction on a standard BEM solution with Prandtl tip loss and Glauert high-load correction: after the induction iteration has converged, the additional driving force per blade of a section tilted by $\kappa = \arctan(\mathrm{d}z_{oop}/\mathrm{d}r)$ is computed from the Kutta–Joukowski theorem with bound circulation $\Gamma = \frac{1}{2} W c\, c_L$,

$$\mathrm{d}F_{z,inc} = \rho\,\Gamma\, u_r \tan(\kappa)\,\mathrm{d}r\ , \qquad (1)$$

i.e. a one-way coupling in the nomenclature of Li et al. (2022); the axial momentum balance is left untouched, so thrust is identical in all variants by construction.

https://doi.org/10.5194/wes-2026-138
Preprint. Discussion started: 3 September 2026

Model 1 (Madsen). The radial induced velocity is taken as the exact logarithmic form of Eq. (6) of Li et al. (2022),

$$u_r(x) = \frac{U_0}{2.24}\,\frac{c_{T,av}}{4\pi}\ln\left[\frac{0.04^2+(x+1)^2}{0.04^2+(x-1)^2}\right], \qquad x = r/R\,, \tag{2}$$

driven by the area-averaged thrust coefficient $c_{T,av}(r) = \int_0^r c_T\, 2\pi r^* \mathrm{d}r^*/(\pi r^2)$.

Model 2 (vortex cylinder). The converged inductions a_i of the N_{sec} annuli define $N_{sec}+1$ semi-infinite right cylinders of strength $\gamma_t^{(k)} = 2U_0(a_k - a_{k-1})$ (ghost values $a_0 = a_{N+1} = 0$) located at the annulus boundaries R_k and starting at the axial position of the deflected blade. Each cylinder induces (Branlard and Gaunaa, 2015)

$$u_r(r,x) = -\frac{\gamma_t}{2\pi}\sqrt{\frac{R_k}{r}}\left[\frac{2-k^2}{k}K(k^2) - \frac{2}{k}E(k^2)\right], \qquad k^2 = \frac{4rR_k}{(R_k+r)^2+x^2}\,, \tag{3}$$

with complete elliptic integrals K and E; the total u_r at a blade section is the superposition over all cylinders. In the FORTRAN implementation K and E are evaluated by the polynomial approximations 17.3.34–37 of Abramowitz and Stegun (1964); a Python replica using double-precision routines from scipy reproduces the FORTRAN result to $2\times10^{-2}\,\mathrm{m\,s^{-1}}$ and is used for the grid study below.

3 Results

3.1 NREL 5 MW reference rotor

Table 1 summarises the effect for the NREL 5 MW baseline rotor (Jonkman et al., 2009) at $11\,\mathrm{m\,s^{-1}}$, 12.1 rpm, zero pitch, $N_{sec} = 70$, with an assumed operational tip deflection of 6 m ($\kappa \approx 5.7°$ along the blade). Both models increase the power by a driving moment of +62 kNm ($\Delta c_P/c_P \approx +0.2\,\%$ at this small κ); the difference between the two models in Δc_P is a factor of 30 smaller than the correction itself.

Table 1: Effect of radial induction, NREL 5 MW baseline, 11 m $\mathrm{s^{-1}}$, 6 m tip deflection.

	planar	Madsen	vortex cylinder
Thrust / kN	699.8	695.1	695.1
Power / kW	4718.4	4726.3	4728.7
c_P	0.4642	0.4649	0.4652

Figure 1 compares the local distributions. The two models agree in magnitude over the outer half of the blade (within 10–35 % for $0.7 < r/R < 0.92$), but disagree qualitatively elsewhere: at mid-span the VC result changes sign, following the non-monotonic $a(r)$ of the BEM solution ($\gamma_t \propto \Delta a$), which the smooth $c_{T,av}$-driven Madsen fit cannot represent; towards the tip the VC value at the outermost section reaches $6.6\,\mathrm{m\,s^{-1}}$ against $2.3\,\mathrm{m\,s^{-1}}$.

3.2 Grid dependence of the tip value

To isolate the discretisation behaviour of the VC superposition, the converged $a(r)$ of the $N_{sec} = 70$ solution was fixed (cubic spline) and the VC sweep, Eq. (3), repeated on refined grids, $N_{sec} = 35\ldots2240$. Figure 2 shows the result. At any fixed radius $r < R$, u_r converges. The value at the outermost midpoint, however, grows without bound: a fit gives $u_r = 0.78\ln N_{sec} + 3.05$ ($\mathrm{m\,s^{-1}}$), in close agreement with the analytic prediction: the outermost evaluation point approaches the tip cylinder as $\mathrm{d}r/2 \propto 1/N_{sec}$, where $K(k^2) \simeq \frac{1}{2}\ln[16/(1-k^2)]$ and $1-k^2 \propto N_{sec}^{-2}$, so that $u_r \simeq (|\gamma_t^{tip}|/2\pi)\ln N_{sec}$+const with $|\gamma_t^{tip}|/2\pi = 2U_0 a_N/2\pi = 0.82$ $\mathrm{m\,s^{-1}}$ here. The logarithmic edge singularity of the semi-infinite cylinder is thus directly visible numerically.

An implementation detail deserves attention: the FORTRAN code limits the elliptic modulus to $k^2 \leq 1-10^{-6}$, a seemingly innocent numerical guard. Figure 2 (right) shows that this cap becomes active for $N_{sec} \gtrsim 300$ and silently converts the divergence into an N_{sec}-independent plateau at $\approx 7.3\,\mathrm{m\,s^{-1}}$ — an unintended, hidden regularisation. Codes of this class will in general contain such guards, and their effect on tip loads is invisible unless a grid study like the present one is performed.

The Γ-weighted integral, by contrast, is insensitive: the additional driving moment varies only from 62.3 to 61.6 kNm (≈1 %) over the entire range $N_{sec} = 35\ldots2240$, because $\Gamma \to 0$ at the tip suppresses precisely the

https://doi.org/10.5194/wes-2026-138
Preprint. Discussion started: 3 September 2026

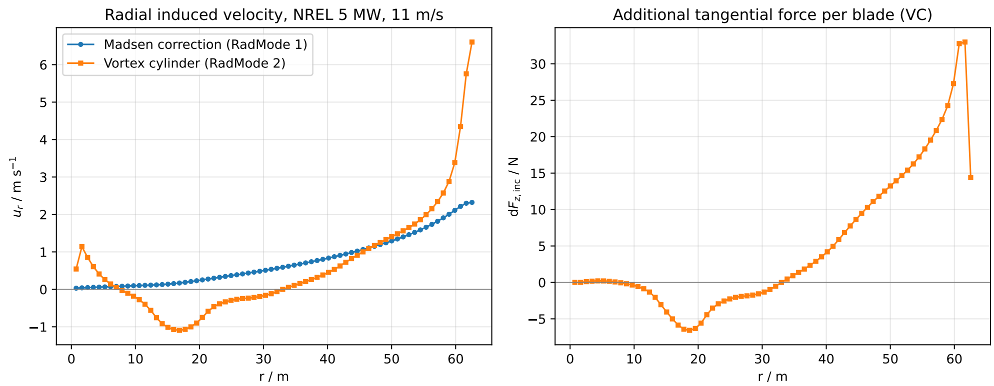

Figure 1: Left: radial induced velocity $u_r(r)$ from both models (NREL 5 MW, 11 m s^{-1}, 6 m tip deflection, $N_{sec} = 70$). Right: additional driving force per blade, Eq. (1), for the VC model.

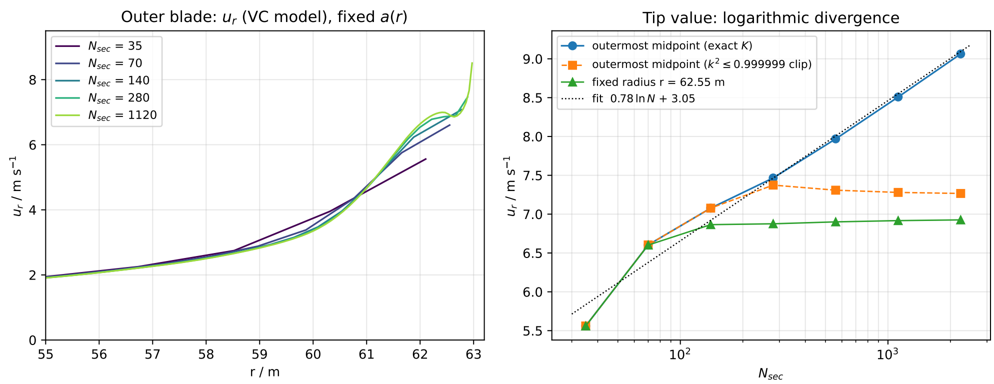

Figure 2: Grid study of the VC sweep with fixed $a(r)$. Left: u_r on the outer blade for increasing N_{sec}. Right: value at the outermost midpoint with exact elliptic integrals (circles), with the implementation guard $k^2 \leq 1 - 10^{-6}$ (squares), and at the fixed radius $r = 62.55$ m (triangles); dotted: logarithmic fit.

divergent region, and the mid-span contributions are small and partially cancelling. This also explains why the two models agree in the integral effect although they disagree locally: the Madsen expression, Eq. (2), is a calibrated fit to the vortex-cylinder flow of the uniformly loaded actuator disc, so wherever the local loading resembles the area average — on the outer half of the blade, which dominates the moment — both models must coincide.

4 Conclusions

For integral quantities (power, thrust) of moderately deflected rotors the Madsen correction and the uncoupled vortex-cylinder model may be used interchangeably; the simpler model is then preferable. Local load predictions near the tip of non-planar rotors, however, are model- and grid-dependent: the discrete VC superposition carries a logarithmic edge singularity that is numerically visible and, in the present implementation, was masked by a hidden numerical guard. Applications that use u_r locally — tip extensions, aeroelastic tailoring, curved winglets — require an explicit, resolution-independent regularisation (e.g. evaluation at annulus centres of a staggered grid, a vortex-core model, or the coupled formulation of Li et al. (2022), Sect. 3.2). A systematic extension to larger prebend angles and to the fully coupled scheme is in preparation.

https://doi.org/10.5194/wes-2026-138
Preprint. Discussion started: 3 September 2026

Code and data availability. The FORTRAN code (KSS, V5), the Python replica of the VC sweep and all input files are available at `https://github.com/Schaffarczyk/KSS/`.

Author contributions. APS: conceptualisation, methodology, writing. BM: implementation preparation, test cases (MSc thesis project). The static code review and the independent reference implementation were carried out with LLM assistance (Anthropic Claude, 2026).

Competing interests. The authors declare no competing interests.

References

Abramowitz, M. and Stegun, I. A.: Handbook of Mathematical Functions, Dover, New York, 1964.

Branlard, E. and Gaunaa, M.: Cylindrical vortex wake model: right cylinder, Wind Energy, 18, 1973–1987, https://doi.org/10.1002/we.1800, 2015.

Glauert, H.: Airplane propellers, in: Aerodynamic Theory, edited by Durand, W. F., Springer, Berlin, 169–360, 1935.

Jonkman, J., Butterfield, S., Musial, W., and Scott, G.: Definition of a 5-MW reference wind turbine for offshore system development, Tech. Rep. NREL/TP-500-38060, NREL, Golden, CO, 2009.

Li, A., Gaunaa, M., Pirrung, G. R., and Horcas, S. G.: A computationally efficient engineering aerodynamic model for non-planar wind turbine rotors, Wind Energ. Sci., 7, 75–104, https://doi.org/10.5194/wes-7-75-2022, 2022.

Madsen, H. Aa., Larsen, T. J., Pirrung, G. R., Li, A., and Zahle, F.: Implementation of the blade element momentum model on a polar grid and its aeroelastic load impact, Wind Energ. Sci., 5, 1–27, https://doi.org/10.5194/wes-5-1-2020, 2020.

Schaffarczyk, A. P., Korjahn, M., and Schlipf, D.: KSS — an open source FORTRAN90 code for aerodynamic design of wind turbine blades, CFD Lab Report No. 128, Kiel University of Applied Sciences, https://github.com/Schaffarczyk/KSS/, 2022 (V5: 2026).